

Scattering statistics in nonlinear wave chaotic systems

Cite as: Chaos 29, 033113 (2019); doi: 10.1063/1.5085653

Submitted: 13 December 2018 · Accepted: 1 February 2019 ·

Published Online: 6 March 2019





View Online



Export Citation



CrossMark

Min Zhou,^{1,2}  Edward Ott,^{1,3} Thomas M. Antonsen, Jr.,^{1,3} and Steven M. Anlage^{1,2,3} 

AFFILIATIONS

¹Department of Electrical and Computer Engineering, University of Maryland, College Park, Maryland 20742, USA

²Center for Nanophysics and Advanced Materials, University of Maryland, College Park, Maryland 20742, USA

³Department of Physics, University of Maryland, College Park, Maryland 20742, USA

ABSTRACT

The Random Coupling Model (RCM) is a statistical approach for studying the scattering properties of linear wave chaotic systems in the semi-classical regime. Its success has been experimentally verified in various over-moded wave settings, including both microwave and acoustic systems. It is of great interest to extend its use in nonlinear systems. This paper studies the impact of a nonlinear port on the measured statistical electromagnetic properties of a ray-chaotic complex enclosure in the short wavelength limit. A Vector Network Analyzer is upgraded with a high power option, which enables calibrated scattering (S) parameter measurements up to +43 dBm. By attaching a diode to the excitation antenna, amplitude-dependent S-parameters and Wigner reaction matrix (impedance) statistics are observed. We have systematically studied how the key components in the RCM are affected by this nonlinear port, including the radiation impedance, short ray orbit corrections, and statistical properties. By applying the newly developed radiation efficiency extension to the RCM, we find that the diode admittance increases with the excitation amplitude. This reduces the amount of power entering the cavity through the port so that the diode effectively acts as a protection element. As a result, we have developed a quantitative understanding of the statistical scattering properties of a semi-classical wave chaotic system with a nonlinear coupling channel.

Published under license by AIP Publishing. <https://doi.org/10.1063/1.5085653>

Many wave systems, ranging from the quantum mechanical wavefunctions of complex molecules to the reverberation of sound in a large concert hall, share a common description in terms of wave chaos. Such systems have been shown to have universal statistical fluctuations governed by the random matrix theory, but their properties are also “dressed” by non-universal features that are specific to each phenomenon. Of particular interest are the scattering properties of wave chaotic systems that are open to the outside world through a finite number of scattering channels. We have developed the Random Coupling Model (RCM) to provide a complete quantitative understanding of all such systems, and we have extended it in several ways to account for increasingly complicated features of such systems. In this paper, we further extend the RCM to understand the amplitude-dependent universal and non-universal properties of a wave chaotic system with a strong nonlinearity built into a coupling channel. Using this extended RCM, we are able to understand the amplitude-dependent experimental data on the scattering properties of a microwave cavity with

a nonlinear diode attached to the scattering port. This is an important step in the ongoing effort to create the science of nonlinear wave chaos.

I. INTRODUCTION

Concepts from the field of wave chaos have been shown to successfully predict the statistical properties of linear fields in enclosures with dimensions much larger than the wavelength. This includes the properties of closed systems, such as eigenvalues and eigenfunctions, as well as the scattering properties of open systems.¹ The Random Coupling Model (RCM) describes the scattering properties by incorporating both universal features described by the Random Matrix Theory (RMT)¹⁻⁷ and the system-specific features of particular system realizations.⁸⁻¹⁰ The RCM is formulated in terms of the Wigner reaction matrix, directly analogous to the electromagnetic or acoustic impedance, rather than the scattering matrix.^{11,12} This allows the RCM to be expanded and appended

in a simple additive or multiplicative manner, creating opportunities to describe increasingly complicated scattering scenarios. Examples of such complications include taking account of “short orbits” between the ports (or scattering channels) that survive the ensemble averaging process^{13–15} and modifications of scattering statistics due to losses localized in the ports, rather than in the scattering system.^{16–18}

Nonlinearity in wave-chaotic systems has been studied in several aspects. For example, rogue waves can appear in linear wave chaotic scattering systems.^{19,20} However, such waves can also appear in a variety of physical contexts and are enhanced by nonlinear mechanisms.^{21,22} In acoustics, Time-Reversed Nonlinear Elastic Wave Spectroscopy (TR/NEWS) is based on the nonlinear time reversal properties of a wave chaotic system.²³ TR/NEWS is proposed as a tool to detect micro-scale damage features (e.g., delaminations, micro-cracks, or weak adhesive bonds) via their nonlinear acoustic signatures.^{24,25} Applying this idea to electromagnetic waves,²⁶ the nonlinear electromagnetic time-reversal mirror shows promise for novel applications such as exclusive communication and wireless power transfer.^{27–30} The theoretical study of stationary scattering from quantum graphs has been generalized to the nonlinear domain, where the nonlinearity creates multi-stability and hysteresis.³¹ A wave-chaotic microwave cavity with a nonlinear circuit feedback loop demonstrated sub-wavelength position sensing for a perturber inside the cavity.³² Nonlinearity is a key ingredient in various machine learning protocols, including neural networks^{33,34} and reservoir computing.^{35,36} Utilizing wave chaotic layers, along with nonlinearity, offers an attractive way to enable physical realizations of deep learning machines.^{37–39}

Nonlinear effects in wave chaotic systems manifest as harmonic and sub-harmonic generation, driving amplitude dependent responses, etc. We have recently studied the statistics of harmonics generated in a wave chaotic system by adding an active frequency multiplier to the 1/4-bowtie microwave billiard,⁴⁰ which is a vertically thin (less than a half-wavelength) microwave cavity whose horizontal shape resembles a quarter of a bowtie (Fig. 1). This is quite relevant to the work that investigates the electromagnetic field statistics created by nonlinear electronics inside a wave chaotic reverberation chamber, and it has a number of applications in the EMC (Electromagnetic Compatibility) community, such as the electromagnetic immunity testing of digital electronics.^{41,42} Another approach to observe the nonlinear effects is to create a scattering system with amplitude dependent response. To achieve this, we have introduced different sources of nonlinearity into the billiards, and in this paper, we focus on a high frequency diode. Reaching the nonlinear regime usually requires high amplitude inputs, hence we have implemented a high power vector network analyzer (VNA) which is able to measure the scattering (S) parameters for signals up to $\sim +43$ dBm (≈ 20 W).

In this paper, we first briefly review the salient features of the Random Coupling Model and several of its extensions. We then discuss the microwave billiard experiment with a nonlinear diode element attached to the single port. The raw data are

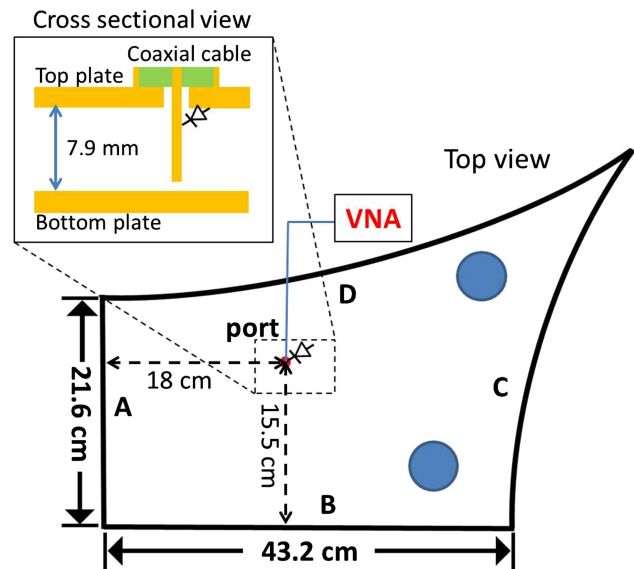


FIG. 1. Top view of the experimental setup of the 1/4-bowtie quasi-2D microwave billiard loaded with a diode attached to the single port. The diode (Infineon BAS7004) is connected between the center pin of the port and the top plate. The antenna pin is 7.6 mm long and 1.27 mm in diameter. The diode package has a dimension of $1.3 \times 2.9 \times 1$ mm³. The Vector Network Analyzer (Keysight N5242A PNA-X) measures the scattering parameter at excitation levels up to +43 dBm with microwave wavelengths from 3 to 7.5 cm. The two blue solid circles are metallic perturbers that can be moved around to create ensemble realizations. The inset shows a side-view cross section through the diode-loaded antenna.

presented and discussed, and then a nonlinear generalization of the RCM is presented and applied to the data. The results are discussed and conclusions are drawn in Sec. VI.

II. RCM OVERVIEW

The basic idea of the RCM is as follows. For an N -port ray chaotic system, the statistical properties of the $N \times N$ cavity impedance matrix $\bar{\bar{Z}}_{cav}$ are described by a universally fluctuating complex normalized impedance $\bar{\bar{\xi}}$ and the system specific properties $\bar{\bar{Z}}_{avg}$ through the following equation:^{9,10,13–15}

$$\bar{\bar{Z}}_{cav} = i \cdot \text{Im}\{\bar{\bar{Z}}_{avg}\} + [\text{Re}\{\bar{\bar{Z}}_{avg}\}]^{1/2} \cdot \bar{\bar{\xi}} \cdot [\text{Re}\{\bar{\bar{Z}}_{avg}\}]^{1/2}, \quad (1)$$

where $\bar{\bar{Z}}_{avg}$ is the average impedance over an ensemble of cavity realizations. $\bar{\bar{Z}}_{avg}$ contains the non-universal features of the system, including the radiation impedance of the port (which fully characterizes the port-specific properties that determine the “prompt response” to an input excitation^{8,13,14,43,68}), and short orbits that survive the ensemble average.^{13–15} The “radiation impedance” $\bar{\bar{Z}}_{rad}$ describes the impedance of the port when only outgoing waves are present. Practically speaking, it is measured in the case that the waves get into the cavity through the port but do not return. This can be realized, for example, by covering the boundary of the billiard with perfect

microwave absorbers. A “short orbit” describes a ray trajectory that leaves the port and immediately returns to it, or another port, without ergodically visiting the chaotic system. It is the result of the port-to-port interaction that introduces deterministic field components which can remain fixed in the ensemble.¹⁴ Under the assumption that losses are uniform, the statistics of the universally fluctuating complex impedance $\bar{\xi}$ is determined by a single parameter named the loss parameter α .^{8,9,43,44} For a two-dimensional electromagnetic system (i.e., a vertically thin cavity), it is given by $\alpha = k^2 A / (4\pi Q)$ and can be interpreted as the ratio of the typical 3-dB bandwidth of the resonant modes to the mean mode spacing. Here, $k = 2\pi f / c$ is the wave number at frequency f , A represents the area of the billiard, and Q is the typical loaded quality factor of the enclosure. The loss parameter α can vary from 0 (isolated resonances) to infinity (many overlapping resonances). The universal statistical properties of a chaotic system with loss parameter α is given by RMT.^{9,10,45–47} Note that we can invert Eq. (1) and create an experimental approximate to the statistics of $\bar{\xi}$, called $\bar{\xi}_{exp}$ by gathering an ensemble of \bar{Z}_{cav} , and constructing \bar{Z}_{avg} . By fitting the statistics of $\bar{\xi}_{exp}$ to theoretical predictions, the loss parameter of the system can be estimated.

The success of the principles underlying the RCM has been experimentally verified in linear wave chaotic systems including microwave systems^{48–50} and acoustic systems,^{51–55} from 1D quantum graphs,^{56–58} 2D electromagnetic billiards,^{14,15,43,59} and 3D cavities.^{60–63} Based on its success and flexibility, it is of great interest to extend the RCM to other systems. One area of extension is to nonlinear systems.

In this work, we show the results for measurements of the nonlinear scattering parameters in a diode-loaded 1/4-bowtie quasi two-dimensional microwave cavity. The 1/4-bowtie cavity is a ray-chaotic billiard that displays universal statistical properties predicted by RMT and RCM.^{9,10,45,49,64–70} In this case, the diode acts as a nearly point-like nonlinearity in a wave chaotic system. Attaching a diode to the excitation port, we observed that the raw cavity statistics of the impedance change substantially with the excitation power. We extend the RCM to this situation and use it to analyze our experimental results. We find that when the radiation impedance becomes nonlinear, short orbits between the port and a nearby wall, and the raw impedance statistics are strongly modified. We also find that many of these changes are due to the fact that the admittance of the diode changes with the excitation power. The nonlinear diode competes with the cavity admittance, substantially altering the response of the system. By implementing the lossy port model extension of the RCM,^{16–18} the results are well explained by the changing radiation efficiency of the diode-loaded port. As a result, the diode effectively acts like a protection element in this configuration.

III. EXPERIMENTAL SETUP

In the small signal limit, our system can be approximated as linear. To observe a nonlinear response, the system must

have some sort of nonlinear property, and a large excitation signal is required. In our earlier studies of wave chaotic systems with one port or multiple ports, we measured the scattering parameters and used these measurements to study the statistical properties of the system. Here, we measure the high power S-parameters including a nonlinear element in the wave system, at power levels up to +43 dBm (see the [supplementary material](#)).

To induce strong nonlinearity, a diode (Infineon BAS7004 with two diodes in the package but only one is electrically connected) is soldered between the center pin and cavity ground, as shown in the inset to Fig. 1. From the datasheet,⁷¹ this diode has low transition capacitance, $C \sim 1.5$ pF at 1 MHz, which decreases nonlinearly to ~ 0.5 pF as the reverse voltage increases. Its differential resistance also changes nonlinearly as a function of the forward current. For typical forward currents $I_F = 1 \sim 15$ mA, the resistance R changes from 80 to 20 Ω . A rough estimate for the time constant $\tau_{RC} = RC \sim 100$ ps, which is close to the charge carrier life-time as given in the data sheet. Thus, this diode can respond in the GHz frequency range and produce clear nonlinear responses, making it suitable for our microwave wave chaos experiments.^{72,73} In addition, the diode package is significantly smaller than the wavelengths used in this study (30–75 mm), rendering it approximately “point like.” The connection shown in Fig. 1 has advantages in terms of stability and reproducibility, due to the fact that when the bowtie billiard is opened, the antenna and the top plate are attached together as one piece, and the bottom plate is a separate piece. This in turn allows for excellent reproducibility of \bar{Z}_{rad} (radiation impedance, see the [supplementary material](#)), \bar{Z}_{cav} , and \bar{Z}_{avg} measurements.

IV. RESULTS

With this diode loaded nonlinear port, we observed that both the system specific properties and universal statistics change dramatically with the input microwave amplitude. The detailed analysis of the system specific properties, including the radiation impedance and short orbits, is presented in the [supplementary material](#). Here, we focus mainly on the scattering statistics, which are significantly affected in the 4 ~ 10 GHz range.

A. Ensemble realizations

To analyze the statistics of the cavity, the metallic perturbors shown in Fig. 1 are moved around to create 120 distinct static realizations. Figure 2(a) shows reflection vs. frequency results for a typical realization for low (blue) and high (green) input power. They have similar shapes as in the radiation case, but are “decorated” with many resonance fluctuations. The linear RCM approach applies well in the low power case, and we follow the RCM normalization process to determine an experimental approximate, ξ_{exp} .^{8,10,14} Figure 2(b) shows PDFs of $Re(\xi_{exp})$ in the 6.5 to 7.5 GHz range for several different input powers. Clearly, the PDF of the normalized impedance $Re(\xi_{exp})$ changes substantially with power, being more widely

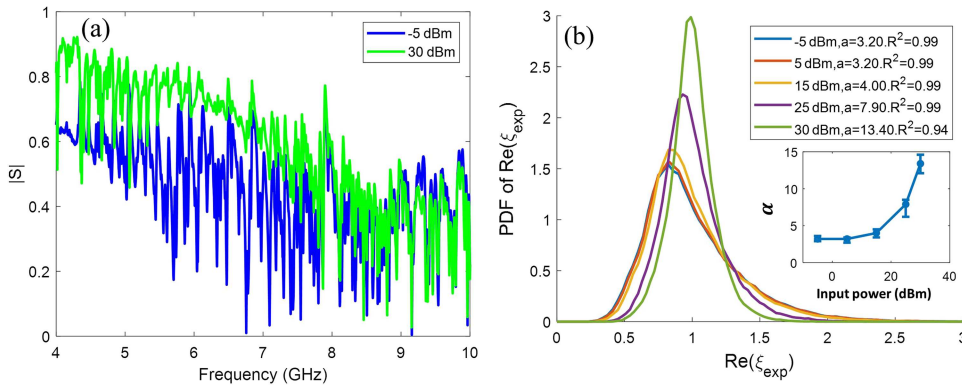


FIG. 2. (a) Comparing the reflection S-parameter $|S|$ of a typical single realization of the 1/4-bowtie cavity with a diode-loaded port for low power (blue, -5 dBm) and high power (green $+30$ dBm). (b) Histogram of normalized $Re(\xi_{exp})$ obtained from ensemble data using traditional linear RCM for a 1 GHz window centered at 7 GHz. The resulting fitted loss parameter α increases with power as shown in the inset. R^2 values in the legend indicate the goodness of fit.⁴⁰

distributed in the low power case, indicating stronger fluctuations, a property which is associated with lower loss parameter α . Note that the $Re(\xi_{exp})$ distribution is more concentrated near unity as power increases, consistent with a high loss (high α) situation. If we naively fit this distribution function to the RCM prediction using α as the sole fitting parameter, the fitted loss parameter α systematically increases with power, as shown in the inset. The raw statistics of the system change substantially with power because of the presence of the nonlinear port. However, it should be noted that these ξ_{exp} PDFs show substantial deviations from RMT predictions (note the low fit R^2 values at high power), making it clear that the naive application of the RCM breaks down in the nonlinear regime.

B. Radiation efficiency of the nonlinear port (high loss system)

In the RCM treatment presented above, we expect the loss parameter of the system to be independent of the excitation power as long as the properties of the cavity remain unchanged. The nonlinear property in this case is only associated with the port. The RCM described in Eq. (1) is derived assuming a lossless linear port. But this is no longer the case in this experiment. As we can see from Fig. 2(a) particularly in the vicinity of 6 GHz, the fluctuations are suppressed in the high power case, indicating that excitations of the cavity modes are suppressed. In this case, the port must be considered as a lossy port. References 16 and 17 have derived a generalization of the RCM to account for the loss of the port. A radiation efficiency η is introduced to quantify the ratio of the power radiated by the port to the input power to the antenna, $\eta = P_{rad}/P_{in}$ (η is real and $0 \leq \eta \leq 1$). In a high loss system (i.e., $\alpha \gg 1$), it can be shown that the impedance of a lossy antenna inside a complex enclosure can be approximated as

$$\bar{\bar{Z}}_{in} = \bar{\bar{Z}}_{ant} + \eta \cdot Re\{\bar{\bar{Z}}_{ant}\} \cdot \delta\bar{\bar{\xi}}, \tag{2}$$

where η is the radiation efficiency of the antenna, $\delta\bar{\bar{\xi}} = \bar{\bar{\xi}} - \bar{\bar{I}}$, $\bar{\bar{I}}$ is the identity matrix with diagonal elements $1 + i0$, and $\bar{\bar{Z}}_{ant}$ is the input impedance of the lossy antenna radiating in free space. Reference 18 has successfully applied this model to a scaled cavity, where the radiation efficiency accounts for

the loss in free-space propagation suffered through a remote injection path. In our case, $\bar{\bar{Z}}_{in}$ can be considered as $\bar{\bar{Z}}_{cav}$ and $\bar{\bar{Z}}_{ant}$ can be considered as $\bar{\bar{Z}}_{avg}$, therefore, Eq. (2) can be modified as

$$\bar{\bar{Z}}_{cav} = i \cdot Im\{\bar{\bar{Z}}_{avg}\} + (\bar{\bar{I}} + \eta \cdot \delta\bar{\bar{\xi}}) \cdot Re\{\bar{\bar{Z}}_{avg}\}, \tag{3}$$

which is valid in the limit $\alpha \gg 1$. To determine η for the nonlinear port, we first measure $\bar{\bar{\xi}}_{cav}$ of the billiard when there is no diode attached to the antenna. In that case, $\bar{\bar{\xi}}_{cav}$ describes the properties of the billiard alone (because all system-specific properties have been removed), and as such it is a linear system. We use the linear RCM approach, creating 120 realizations with the two perturbers, then applying Eq. (1) to extract $\bar{\bar{\xi}}_{cav}$ and fit to RCM to find the corresponding loss parameter α .^{8,10,14} Additionally, to make the bowtie billiard a high loss system, the perimeter of the billiard is partly (but uniformly) covered with microwave absorbers, tuning the loss parameter to be $\alpha = 3$ (4.5 GHz) to $\alpha = 7$ (9.5 GHz). Then, using the value of α which characterizes loss in the cavity and $\bar{\bar{\xi}}_{cav}$, we go back to the diode-loaded nonlinear port case, utilizing Eq. (3) and varying η so that the statistics of $\bar{\bar{\xi}}(\eta)$ agree with $\bar{\bar{\xi}}_{cav}$. Figure 3(a) shows the fitted radiation efficiency from $Im(\xi)$ statistics [the $Re(\xi)$ statistics give similar results].

Figure 3(a) shows that the radiation efficiency is strongly power-dependent in the frequency range 4 ~ 10 GHz. Between 6 and 9 GHz, the radiation efficiency decreases with increasing power, meaning the port is getting more lossy as the excitation power increases. There is a cross-over regime at a low frequency of 4 ~ 6 GHz, where the radiation efficiency increases at high powers. And although it is not shown in the plot, at 10 GHz and above, the radiation efficiency is almost independent of power.

To explain the results, we are interested in characterizing the diode admittance under different excitation powers. The diode is connected between the center pin and the ground of the port. The billiard radiation admittance can also be considered as being connected between the center pin and ground. Therefore, a simple model is constructed by considering the diode and the billiard to be connected in parallel. By measuring the port radiation admittance with ($Y_{with\ diode}^{rad}$) and without

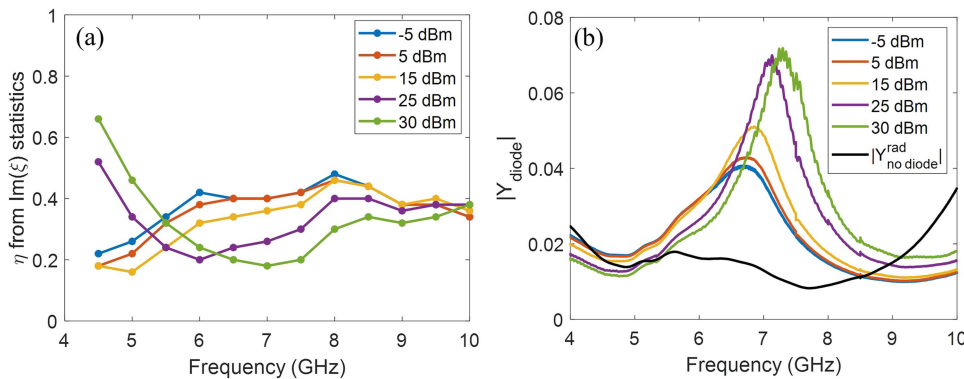


FIG. 3. (a) Fitted radiation efficiency η [from $Im(\xi)$ statistics] versus frequency and power. Each fit was done with data from 120 realizations and a window of 1 GHz. (b) Plot of diode admittance magnitude versus frequency at various rf powers, as well as the radiation admittance of the linear port $|Y_{no diode}^{rad}|$.

the diode ($Y_{no diode}^{rad}$), the diode admittance can be approximated as $Y_{diode} \simeq Y_{with diode} - Y_{no diode}^{rad}$.

Figure 3(b) shows the experimental results of $|Y_{diode}|$ compared with $|Y_{no diode}^{rad}|$. Between 4 and 6 GHz, $|Y_{diode}|$ has similar values to $|Y_{no diode}^{rad}|$ and changes little with power. Thus, the diode admittance competes roughly equally with the billiard admittance. A small change in the admittance value may result in a big change in the fitted radiation efficiency. However, between 6 and 9 GHz, the diode admittance dominates the billiard admittance and generally increases with power. In this frequency range, because the diode admittance is much larger than the billiard admittance and increases with power, the radiation efficiency of the port decreases, consistent with the results in Fig. 3(a).

To better understand the nonlinear port, we built a circuit model for simulation in the finite difference time-domain code called CST (Computer Simulation Technology). The SPICE models of the diode as well as the package are provided by the manufacturer. In addition to the SPICE models, the dielectric properties of the package near the port also affect the radiation impedance, and this was added to the model. The internal capacitances of the package SPICE model were altered because the diode is being used beyond its design frequency range. The simulated amplitude dependent radiation S-parameters show relatively good agreement with the experimental results (see the [supplementary material](#)). In addition, the resultant radiation efficiency that is directly calculated as P_{rad}/P_{in} is in general agreement with the experimental results. Based on the circuit model, the nonlinearity arises from the diode, which is approximated with an exponential I-V diode function.⁷⁴ The diode nonlinearity is shorted by parasitic capacitance in the package SPICE model at high frequencies, thus the port model does not have power dependence at 10 GHz and above, consistent with the data.

V. DISCUSSION AND FUTURE WORK

We have shown that by attaching a diode to the center pin and ground of an antenna, the port shows dramatic nonlinear behavior. For the statistical results, if we blindly apply the RCM to the billiard with a diode-loaded port, one finds that the loss parameter increases with the input power. The

RCM posits that the loss parameter determines the universal properties of the chaotic system. In our case, the billiard properties should not change with power because the nonlinearity is only associated with the port. We applied the newly developed radiation efficiency model to the port, using the radiation efficiency η to quantify the proportion of power from the source radiated into the billiard. At high power in the nonlinear region, the diode consumes most of the power, causing the radiation efficiency to decrease. The diode thus prevents high power signals from getting into the billiard.⁷⁵

There are several interesting questions for further study of this system. First, the billiard had to be intentionally modified into a high loss system in order to use the radiation efficiency model. The statistics of low-loss nonlinear systems cannot be addressed at this time. In addition, another behavior we have observed is the loss of reciprocity in a two-port version of this system, where one port is a nonlinear port and the other is linear. We observed that $S_{12} \neq S_{21}$ when large amplitude signals are applied. We note that there is no general reciprocity theorem that holds for nonlinear systems.⁷⁶ This behavior can be understood by considering that with equal powers injected in both ports, the diode will be driven to nonlinearity when power is injected in the port hosting the diode, and to a lesser extent when the linear port is excited.

Besides the approach we used in this paper to analyze the nonlinear system, we mention for completeness that high power S-parameters are sometimes called hot S-parameters,⁷⁷ and the nonlinear effects can be fully characterized by the so-called X-parameters measured by the nonlinear VNA.^{78,79} However, we believe that the present treatment is best suited for understanding the statistical properties of nonlinear wave chaotic systems in the semi-classical regime.

VI. CONCLUSIONS

To conclude, a diode based nonlinear port alters the radiation impedance, short orbits, and raw impedance statistics of a wave chaotic system from those observed in a linear system. By using the Random Coupling Model with incorporation of the diode nonlinear properties and a lossy port model, these nonlinear phenomena are well explained and verified by the simulation. The nonlinear property of the port can be applied

to protect delicate circuits from high power electromagnetic microwave interference. This represents an important step forward in understanding the statistical scattering properties of a semi-classical wave chaotic system with a nonlinear coupling channel. The raw data are available in Ref. 80.

SUPPLEMENTARY MATERIAL

The [supplementary material](#) contains more information on the implementation of high-power vector network analyzer (VNA), detailed analysis of the nonlinear effects on the system specific properties, and simulation results of the diode-loaded port in computer simulation technology (CST).

ACKNOWLEDGMENTS

This work is supported by the AFOSR under COE Grant No. FA9550-15-1-0171, the ONR under Grant No. N000141512134, the COST Action IC1407 "ACCREDIT" supported by COST (the European Cooperation in Science and Technology), and the Maryland Center for Nanophysics and Advanced Materials (CNAM).

REFERENCES

- ¹H. J. Stöckmann, *Quantum Chaos: An Introduction* (Cambridge University Press, Cambridge, 1999).
- ²G. Casati, F. Valz-Gris, and I. Guarneri, "On the connection between quantization of nonintegrable systems and statistical theory of spectra," *Lett. Nuovo Cimento* **28**, 279 (1980).
- ³O. Bohigas, M. J. Giannoni, and C. Schmit, "Characterization of chaotic quantum spectra and universality of level fluctuation laws," *Phys. Rev. Lett.* **52**, 1–4 (1984).
- ⁴C. W. J. Beenakker, "Random-matrix theory of quantum transport," *Rev. Mod. Phys.* **69**, 731 (1997).
- ⁵T. Guhr, A. Müller-Groeling, and H. A. Weidenmüller, "Random-matrix theories in quantum physics: common concepts," *Phys. Rep.* **299**, 189 (1998).
- ⁶Y. Alhassid, "The statistical theory of quantum dots," *Rev. Mod. Phys.* **72**, 895 (2000).
- ⁷F. Haake, *Quantum Signatures of Chaos*, 2nd ed. (Springer, Berlin, 2000).
- ⁸S. Hemmady, X. Zheng, E. Ott, T. M. Antonsen, and S. M. Anlage, "Universal impedance fluctuations in wave chaotic systems," *Phys. Rev. Lett.* **94**, 014102 (2005).
- ⁹X. Zheng, T. M. Antonsen, and E. Ott, "Statistics of impedance and scattering matrices in chaotic microwave cavities: Single channel case," *Electromagnetics* **26**, 3 (2006); X. Zheng, T. M. Antonsen, Jr., and E. Ott, "Statistics of impedance and scattering matrices of chaotic microwave cavities with multiple ports," *Electromagnetics* **26**, 37 (2006).
- ¹⁰G. Gradoni, J.-H. Yeh, B. Xiao, T. M. Antonsen, S. M. Anlage, and E. Ott, "Predicting the statistics of wave transport through chaotic cavities by the random coupling model: A review and recent progress," *Wave Motion* **51**, 606–621 (2014).
- ¹¹F. Beck, C. Dembowski, A. Heine, and A. Richter, "R-matrix theory of driven electromagnetic cavities," *Phys. Rev. E* **67**, 066208 (2003).
- ¹²G. E. Mitchell, A. Richter, and H. A. Weidenmüller, "Random matrices and chaos in nuclear physics: Nuclear reactions," *Rev. Mod. Phys.* **82**, 2845 (2010).
- ¹³J. A. Hart, T. M. Antonsen, and E. Ott, "The effect of short ray trajectories on the scattering statistics of wave chaotic systems," *Phys. Rev. E* **80**, 041109 (2009).
- ¹⁴J.-H. Yeh, J. Hart, E. Bradshaw, T. Antonsen, E. Ott, and S. M. Anlage, "Universal and non-universal properties of wave chaotic scattering systems," *Phys. Rev. E* **81**, 025201(R) (2010).
- ¹⁵J.-H. Yeh, J. Hart, E. Bradshaw, T. Antonsen, E. Ott, and S. M. Anlage, "Experimental examination of the effect of short ray trajectories in two-port wave-chaotic scattering systems," *Phys. Rev. E* **82**, 041114 (2010).
- ¹⁶B. D. Addissie, J. C. Rodgers, and T. M. Antonsen, Jr., "Application of the random coupling model to lossy ports in complex enclosures," in *2015 IEEE Metrology for Aerospace (MetroAeroSpace)*, Benevento (IEEE, 2015), pp. 214–219.
- ¹⁷B. D. Addissie, J. C. Rodgers, and T. M. Antonsen, "Extraction of the coupling impedance in overmoded cavities," *Wave Motion* (to be published).
- ¹⁸B. Xiao, T. M. Antonsen, E. Ott, Z. B. Drikas, J. G. Gil, and S. M. Anlage, "Revealing underlying universal wave fluctuations in a scaled ray-chaotic cavity with remote injection," *Phys. Rev. E* **97**, 062220 (2018).
- ¹⁹E. J. Heller, L. Kaplan, and A. Dahlen, "Refraction of a Guassian seaway," *J. Geophys. Res.* **113**, C09023 (2008).
- ²⁰R. Höhmann, U. Kuhl, H.-J. Stöckmann, L. Kaplan, and E. J. Heller, "Freak waves in the linear regime: A microwave study," *Phys. Rev. Lett.* **104**, 093901 (2010).
- ²¹K. Dysthe, H. E. Krogstad, and P. Müller, "Oceanic rogue waves," *Annu. Rev. Fluid Mech.* **40**, 287–310 (2008).
- ²²M. Onorato, S. Residori, U. Bortolozzo, A. Montina, and F. T. Arecchi, "Rogue waves and their generating mechanisms in different physical contexts," *Phys. Rep.* **528**, 47 (2013).
- ²³B. Van Damme, K. Van Den Abeele, Y. F. Li, and O. B. Matar, "Time reversed acoustics techniques for elastic imaging in reverberant and nonreverberant media: An experimental study of the chaotic cavity transducer concept," *J. Appl. Phys.* **109**(10), 104910 (2011).
- ²⁴R. Guyer and P. Johnson, "Nonlinear mesoscopic elasticity: Evidence for a new class of materials," *Phys. Today* **52**(4), 30 (1999).
- ²⁵K. E. A. Van Den Abeele, A. Sutin, J. Carmeliet, and P. A. Johnson, "Micro-damage diagnostics using nonlinear elastic wave spectroscopy (NEWS)," *NDT E Int.* **34**(4), 239–248 (2001).
- ²⁶G. Lerosee, J. de Rosny, A. Tourin, and M. Fink, "Focusing beyond the diffraction limit with far-field time reversal," *Science* **315**, 1120 (2007).
- ²⁷M. Frazier, B. Taddese, T. Antonsen, and S. M. Anlage, "Nonlinear time-reversal in a wave chaotic system," *Phys. Rev. Lett.* **110**, 063902 (2013).
- ²⁸M. Frazier, B. Taddese, B. Xiao, T. Antonsen, E. Ott, and S. M. Anlage, "Non-linear time reversal of classical waves: Experiment and model," *Phys. Rev. E* **88**, 062910 (2013).
- ²⁹F. Cangialosi, T. Grover, P. Healey, T. Furman, A. Simon, and S. M. Anlage, "Time reversed electromagnetic wave propagation as a novel method of wireless power transfer," in *2016 IEEE Wireless Power Transfer Conference (WPTC)*, Aveiro (IEEE, 2016), pp. 1–4.
- ³⁰S. Roman, R. Gogna, and S. M. Anlage, "Selective collapse of nonlinear time reversed electromagnetic waves," in *2016 IEEE Wireless Power Transfer Conference (WPTC)*, Aveiro (IEEE, 2016), pp. 1–4.
- ³¹S. Gnuzmann, U. Smilansky, and S. Derevyanko, "Stationary scattering from a nonlinear network," *Phys. Rev. A* **83**, 033831 (2011).
- ³²S. D. Cohen, H. L. D. de S. Cavalcante, and D. J. Gauthier, "Subwavelength position sensing using nonlinear feedback and wave chaos," *Phys. Rev. Lett.* **107**, 254103 (2011).
- ³³Y. LeCun, Y. Bengio, and G. Hinton, "Deep learning," *Nature* **521**, 436–444 (2015).
- ³⁴G. Satat, M. Tancik, O. Gupta, B. Heshmat, and R. Raskar, "Object classification through scattering media with deep learning on time resolved measurement," *Opt. Express* **25**, 17466–17479 (2017).
- ³⁵J. Pathak, Z. Lu, B. R. Hunt, M. Girvan, and E. Ott, "Using machine learning to replicate chaotic attractors and calculate Lyapunov exponents from data," *Chaos* **27**, 121102 (2017).
- ³⁶J. Pathak, B. Hunt, M. Girvan, Z. Lu, and E. Ott, "Model-free prediction of large spatiotemporally chaotic systems from data: A reservoir computing approach," *Phys. Rev. Lett.* **120**, 024102 (2018).

- ³⁷Y. Shen, N. C. Harris, S. Skirlo, M. Prabhu, T. Baehr-Jones, M. Hochberg, X. Sun, S. Zhao, H. Larochelle, D. Englund, and M. Soljačić, “Deep learning with coherent nanophotonic circuits,” *Nat. Photonics* **11**, 441 (2017).
- ³⁸S. Rotter and S. Gigan, “Light fields in complex media: Mesoscopic scattering meets wave control,” *Rev. Mod. Phys.* **89**, 015005 (2017).
- ³⁹P. del Hougne, M. Fink, and G. Lerosey, “Shaping microwave fields using nonlinear unsolicited feedback: Application to enhance energy harvesting,” *Phys. Rev. Appl.* **8**, 061001 (2017).
- ⁴⁰M. Zhou, E. Ott, T. M. Antonsen, and S. M. Anlage, “Nonlinear wave chaos: statistics of second harmonic fields,” *Chaos* **27**, 103114 (2017).
- ⁴¹I. Flintoft, A. Marvin, and L. Dawson, “Statistical response of nonlinear equipment in a reverberation chamber,” in *2008 IEEE International Symposium on Electromagnetic Compatibility*, Detroit, MI (IEEE, 2008), pp. 1–6.
- ⁴²L. Guibert, P. Millot, X. Ferrières, and É. Sicard, “An original method for the measurement of the radiated susceptibility of an electronic system using induced electromagnetic nonlinear effects,” *Prog. Electromagn. Res. Lett.* **62**, 83–89 (2016).
- ⁴³S. Hemmady, X. Zheng, T. M. Antonsen, E. Ott, and S. M. Anlage, “Universal statistics of the scattering coefficient of chaotic microwave cavities,” *Phys. Rev. E* **71**, 056215 (2005).
- ⁴⁴S. Hemmady, T. M. Antonsen, Jr., E. Ott, and S. M. Anlage, “Statistical prediction and measurement of induced voltages on components within complicated enclosures: A wave-chaotic approach,” *IEEE Trans. Electromagn. Compat.* **54**, 758–771 (2012).
- ⁴⁵Y. V. Fyodorov and D. V. Savin, “Statistics of impedance, local density of states, and reflection in quantum chaotic systems with absorption,” *JETP Lett.* **80**, 725 (2004).
- ⁴⁶Y. V. Fyodorov, D. V. Savin, and H.-J. Sommers, “Scattering, reflection and impedance of waves in chaotic and disordered systems with absorption,” *J. Phys. A Math. Theor.* **38**, 10731 (2005).
- ⁴⁷H. Li, S. Suwunnarat, R. Fleischmann, H. Schanz, and T. Kottos, “Random matrix theory approach to chaotic coherent perfect absorbers,” *Phys. Rev. Lett.* **118**, 044101 (2017).
- ⁴⁸E. Doron, U. Smilansky, and A. Frenkel, “Experimental demonstration of chaotic scattering of microwaves,” *Phys. Rev. Lett.* **65**, 3072 (1990).
- ⁴⁹P. So, S. M. Anlage, E. Ott, and R. N. Oerter, “Wave chaos experiments with and without time reversal symmetry: GUE and GOE statistics,” *Phys. Rev. Lett.* **74**, 2662 (1995).
- ⁵⁰U. Kuhl, M. Martínez-Mares, R. A. Méndez-Sánchez, and H.-J. Stöckmann, “Direct processes in chaotic microwave cavities in the presence of absorption,” *Phys. Rev. Lett.* **94**, 144101 (2005).
- ⁵¹R. L. Weaver, “Spectral statistics in elastodynamics,” *J. Acoust. Soc. Am.* **85**, 1005 (1989).
- ⁵²C. Ellegaard, T. Guhr, K. Lindemann, H. Q. Lorensen, J. Nygård, and M. Oxborrow, “Spectral statistics of acoustic resonances in aluminum blocks,” *Phys. Rev. Lett.* **75**, 1546 (1995).
- ⁵³Y. Auréan and V. Pagneux, “Acoustic scattering in duct with a chaotic cavity,” *Acta Acust. United Acust.* **102**, 869–875(7) (2016).
- ⁵⁴G. Tanner and Niels Søndergaard, “Wave chaos in acoustics and elasticity,” *J. Phys. A Math. Theor.* **40**, R443 (2007).
- ⁵⁵M. Wright and R. Weaver, *New Directions in Linear Acoustics and Vibration: Quantum Chaos, Random Matrix Theory and Complexity* (Cambridge University Press, 2010).
- ⁵⁶O. Hul, S. Bauch, P. Pakonski, N. Savytsky, K. Zyczkowski, and L. Sirko, “Experimental simulation of quantum graphs by microwave networks,” *Phys. Rev. E* **69**, 056205 (2004).
- ⁵⁷Z. Fu, T. Koch, T. M. Antonsen, E. Ott, and S. M. Anlage, “Experimental study of quantum graphs with simple microwave networks: Non-universal features,” *Acta Phys. Polonica A* **132**(6), 1655–1660 (2017).
- ⁵⁸T. Kottos and U. Smilansky, “Quantum chaos on graphs,” *Phys. Rev. Lett.* **79**, 4794 (1997).
- ⁵⁹H.-J. Stöckmann and J. Stein, “Quantum chaos in billiards studied by microwave absorption,” *Phys. Rev. Lett.* **64**, 2215 (1990).
- ⁶⁰H. Alt, C. Dembowski, H.-D. Gräf, R. Hofferbert, H. Rehfeld, A. Richter, R. Schuhmann, and T. Weiland, “Wave dynamical chaos in a superconducting three-dimensional Sinai billiard,” *Phys. Rev. Lett.* **79**, 1026 (1997).
- ⁶¹Z. B. Drikas, J. G. Gil, S. K. Hong, T. D. Andreadis, J.-H. Yeh, B. T. Taddese, and S. M. Anlage, “Application of the random coupling model to electromagnetic statistics in complex enclosures,” *IEEE Trans. Electromagn. Compat.* **56**, 1480–1487 (2014).
- ⁶²J. G. Gil, Z. Drikas, T. Andreadis, and S. M. Anlage, “Prediction of induced voltages on ports in complex, 3-dimensional enclosures with apertures, using the random coupling model,” *IEEE Trans. Electromagn. Compat.* **58**, 1535–1540 (2016).
- ⁶³X. Li, C. Meng, Y. Liu, E. Schamiloglu, and S. D. Hemmady, “Experimental verification of a stochastic topology approach for high-power microwave effects,” *IEEE Trans. Electromagn. Compat.* **57**(3), 448–453 (2015).
- ⁶⁴A. Gokirmak, D.-H. Wu, J. S. A. Bridgewater, and Steven M. Anlage, “Scanned perturbation technique for imaging electromagnetic standing wave patterns of microwave cavities,” *Rev. Sci. Instrum.* **69**, 3410–3417 (1998).
- ⁶⁵D.-H. Wu, J. S. A. Bridgewater, A. Gokirmak, and S. M. Anlage, “Probability amplitude fluctuations in experimental wave chaotic eigenmodes with and without time reversal symmetry,” *Phys. Rev. Lett.* **81**, 2890–2893 (1998).
- ⁶⁶S.-H. Chung, A. Gokirmak, D.-H. Wu, J. S. A. Bridgewater, E. Ott, T. M. Antonsen, and Steven M. Anlage, “Measurement of wave chaotic eigenfunctions in the time-reversal symmetry-breaking crossover regime,” *Phys. Rev. Lett.* **85**, 2482–2484 (2000).
- ⁶⁷X. Zheng, S. Hemmady, T. M. Antonsen, Jr., S. M. Anlage, and E. Ott, “Characterization of fluctuations of impedance and scattering matrices in wave chaotic scattering,” *Phys. Rev. E* **73**, 046208 (2006).
- ⁶⁸S. Hemmady, X. Zheng, J. Hart, T. M. Antonsen, E. Ott, and S. M. Anlage, “Universal properties of 2-port scattering, impedance and admittance matrices of wave chaotic systems,” *Phys. Rev. E* **74**, 036213 (2006).
- ⁶⁹S. Hemmady, J. Hart, X. Zheng, T. M. Antonsen, Jr., E. Ott, and S. M. Anlage, “Experimental test of universal conductance fluctuations by means of wave-chaotic microwave cavities,” *Phys. Rev. B* **74**, 195326 (2006).
- ⁷⁰J.-H. Yeh, T. M. Antonsen, E. Ott, and S. M. Anlage, “First-principles model of time-dependent variations in transmission through a fluctuating scattering environment,” *Phys. Rev. E* **85**, 015202 (2012).
- ⁷¹Infineon BAS7004 datasheet, see <https://www.infineon.com/cms/en/product/transistor-diode/diode/schottky-diode/high-speed-switching-clipping-and-clamping/bas70-04/>.
- ⁷²R. M. de Moraes and S. M. Anlage, “Unified model and reverse recovery nonlinearities of the driven diode resonator,” *Phys. Rev. E* **68**, 026201 (2003).
- ⁷³R. M. de Moraes and S. M. Anlage, “Effects of UHF stimulus and negative feedback on nonlinear circuits,” *IEEE Trans. Circuits Syst. I* **51**(4), 748–754 (2004).
- ⁷⁴Z. Wu and R. W. Ziolkowski, “Electromagnetic effects associated with a cavity-backed aperture loaded with nonlinear elements,” *Prog. Electromagn. Res.* **28**, 1–16 (2000).
- ⁷⁵R. V. Garver, *Microwave Diode Control Devices* (Artech House, Dedham, MA, 1976).
- ⁷⁶S. Lepri and G. Casati, “Asymmetric wave propagation in nonlinear systems,” *Phys. Rev. Lett.* **106**(16), 164101 (2011).
- ⁷⁷D. S. Dancila et al., “Solid-State Amplifier Development at FREIA,” in *Proceedings of 5th International Particle Accelerator Conference (IPAC'14)*, Dresden, Germany, June 2014, pp. 2282–2284.
- ⁷⁸P. Roblin, *Nonlinear RF Circuits and Nonlinear Vector Network Analyzers: Interactive Measurement and Design Techniques* (Cambridge University Press, Cambridge, UK, 2011).
- ⁷⁹D. E. Root, J. Verspecht, J. Horn, and M. Marcu, *X-Parameters* (Cambridge University Press, Cambridge, 2013).
- ⁸⁰Raw data of Scattering Statistics in Nonlinear Wave Chaotic Systems, see <http://hdl.handle.net/1903/21562>.